


Please cite the Published Version

Yu, Qingping, Shi, Zhiping, Li, Xingwang, Asif, Muhammad, Zhang, Jiayi and Rabie, Khaled 
(2019) Mapping Design for 2M -Ary Bit-Interleaved Polar Coded Modulation. IEEE Access, 7. pp.
116774-116784. ISSN 2169-3536

DOI: <https://doi.org/10.1109/ACCESS.2019.2935791>

Publisher: Institute of Electrical and Electronics Engineers (IEEE)

Version: Published Version

Downloaded from: <https://e-space.mmu.ac.uk/624299/>

Usage rights:  [Creative Commons: Attribution 4.0](https://creativecommons.org/licenses/by/4.0/)

Additional Information: This is an Open Access article published in IEEE Access, published by IEEE, copyright The Author(s).

Enquiries:

If you have questions about this document, contact openresearch@mmu.ac.uk. Please include the URL of the record in e-space. If you believe that your, or a third party's rights have been compromised through this document please see our Take Down policy (available from <https://www.mmu.ac.uk/library/using-the-library/policies-and-guidelines>)

Mapping Design for 2^M -Ary Bit-Interleaved Polar Coded Modulation

QINGPING YU¹, (Student Member, IEEE), ZHIPING SHI¹, (Member, IEEE),
XINGWANG LI², (Member, IEEE), MUHAMMAD ASIF³, (Member, IEEE),
JIAYI ZHANG⁴, (Member, IEEE), AND KHALED M. RABIE⁵, (Member, IEEE)

¹National Key Laboratory of Science and Technology on Communications, University of Electronic Science and Technology of China, Chengdu 611731, China

²School of Physics and Electronic Information Engineering, Henan Polytechnic University, Jiaozuo 454000, China

³Key Laboratory of Wireless-Optical Communication, University of Science and Technology of China, Hefei 230026, China

⁴School of Electronic and Information Engineering, Beijing Jiaotong University, Beijing 100044, China

⁵School of Electrical Engineering, Manchester Metropolitan University, Manchester M1 7JW, U.K.

Corresponding author: Zhiping Shi (szp@uestc.edu.cn)

This work was supported by the National Natural Science Foundation of China under Grant 61671128, Sichuan Science and Technology Program under Grant 2019YFG0105, the Henan Scientific and Technological Research Project under Grant 182102210307, in part by the Fundamental Research Funds for the Universities of Henan Province under Grant NSFRF180309, in part by the Outstanding Youth Science Foundation of Henan Polytechnic University under Grant J2019-4, and in part by the Key Scientific Research Projects of Higher Education Institutions in Henan Province Grant 20A510007.

ABSTRACT This paper proposes a mapping design for bit-interleaved polar coded modulation (BIPCM) systems with belief propagation (BP) decoding. We first introduce a two-layer bipartite graph to represent BIPCM, where a new mapping graph linking polar graph to modulator is added to the conventional factor graph. Then, a mapping design is proposed and the design paradigm is to separate sub-channels with lower reliability to different stopping trees of polar codes, aiming to make sure that each stopping tree receives reliable extrinsic information from demodulator. The proposed mapping algorithm is employed for BIPCM with traditional polar codes over 16-quadrature amplitude modulation (QAM) and 256-QAM. Numerical results show that our scheme can improve the error-correcting performance compared to the conventional scheme with a random mapping. Furthermore, to meet code-length requirement of different modulation orders, we propose an efficient method to construct flexible-length polar code (FLPC) by coupling several short length polar codes with a repeat-accumulate (RA) code. Also, the proposed FLPC is employed in the BIPCM system, with the designed mapping algorithm, simulation result also reveals that the block error rate performance of proposed BIPCM scheme with BP decoding outperforms the one with successive cancellation decoding by providing a gain up to 1 dB.

INDEX TERMS Polar codes, bit-interleaved polar coded modulation (BIPCM), belief propagation decoding.

I. INTRODUCTION

Polar codes, invented by Arıkan in 2009 [1], have been proven to achieve the symmetric capacity of binary-input discrete memoryless channels (BDMCs) with successive cancellation (SC) decoding. Currently, polar codes combined with high-order modulation have become a powerful candidate for the fifth-generation (5G) wireless communication systems with high power and bandwidth efficiencies [2]. For higher spectral efficiency of a practical polar coded system, plenty of works have been done, see e.g. [3]–[7]. Bit-interleaved coded modulation (BICM) proposed in [8] is a practical bandwidth-efficient coding technique. The BICM approach combined with polar codes was introduced in [3].

The associate editor coordinating the review of this article and approving it for publication was Bora Onat.

The authors in [4] provided a mapping searching strategy for bit-interleaved polar coded modulation (BIPCM) based on density evolution (DE). In [5], another mapping strategy was proposed by using auxiliary virtual channels with zero-capacities to avoid exhaustive searching. Furthermore, the authors in [6] extended the channel polarization theorem for multi-channels and proposed a compound polar scheme for 16-quadrature amplitude modulation (QAM) and 64-QAM BICM. In the above BIPCM schemes, SC-based algorithms are used for decoding.

Apart from SC decoding, belief propagation (BP) decoding, proposed in [9], [10] for polar codes based on the factor graph, is also identified as an important decoding method for polar codes. The BP decoding has some fundamental advantages over the SC-based decoding. As it can be easily parallelized, low latency and high throughput

implementations are possible [11]; also it inherently enables soft-in/soft-out decoding, which facilitates joint iterative detection and decoding incorporating techniques such as multiple input multiple output (MIMO) [12], sparse code multiple access (SCMA) [13], and hybrid automatic repeat request (HARQ) [14]. Therefore, it is necessary to design BIPCM with BP decoding for practical communication systems.

In a high-order BICM scheme, as the minimum Euclidean distance for each modulation level is different, all bits within a transmitted symbol get unequal protections from the modulator [15]. A properly designed mapping rule between the encoder and the modulator can lead to significant performance improvement for the BIPCM scheme [3]. Besides, stopping set in the factor graph of code, is an important cause of the decoding failure with BP decoding [16]. In [17], Eslami *et al.* analyzed stopping sets for polar code and their effects on the performance of BP decoding. This property for polar codes over the factor graph has been well utilized to improve the performance of iterative decoding [17]–[21]. Motivated by these observations, in this paper we consider the mapping design for the BIPCM scheme with BP decoding taking both the properties of polar codes over the factor graph and the unequal error protection property of high-order modulations into account.

In this paper, we first introduce a modified factor graph for the polar coded modulation system for a given polar code. Then we propose a mapping design between encoder and modulator for the BIPCM system with BP decoding. Furthermore, to solve the length matching problem between the code length and modulation orders, a novel polar code construction with flexible code length is proposed for the BIPCM scheme. It should be noted that the authors in [22] proposed a BIPCM-ID system under the soft cancellation (SCAN) decoding, in which EXIT chart is applied to code construction for improving the performance. However, the stopping trees are not considered in [22]. The main contributions of this paper are summarized in the following.

- 1) We introduce a two-layer bipartite graph to denote polar coded BICM scheme. Then, we analyze the information transfer process for decoding based on the BIPCM graph.
- 2) For 2^m -ary polar coded modulations, we propose a mapping algorithm to assign coded bits to m bit positions of the transmitted symbols. The proposed mapping takes into account the impact of both unequal error protection of high-order modulator and stopping trees of polar code. Simulation results over additive white Gaussian noise (AWGN) channels show that the designed mapping scheme provides better performance than that of the conventional random mapping scheme, when 16-QAM and 256-QAM are employed.
- 3) To meet the code-length requirements brought by different modulation orders, we introduce a method to construct flexible-length polar code (FLPC), by coupling several short length polar codes with a repeat-accumulate (RA) code. RA code which is

introduced in [23] has simple encoding/decoding structure and low signal noise ratio threshold. Simulation results demonstrate that a combination of the proposed FLPC and the designed mapping with BP decoding provides a frame error rate (FER) performance gain of about 1 dB over the one of the compound polar coded BICM scheme with SC decoding [6], when 64-QAM is implemented over the AWGN channel. With SCAN decoding algorithm, FER performance of the proposed FLPC scheme can outperform the BIPCM scheme with cyclic redundancy check aided successive cancellation list (CASCL) decoding by up to 0.4dB.

The rest of this paper is organized as follows. In Section II, some background on polar coding, decoding as well as stopping trees is provided. In Section III, we introduce the BIPCM system model and describe the proposed mapping design. In Section IV, a constructing method for polar codes with flexible code length is proposed. Simulation results are presented and discussed in Section V. Finally, conclusions are drawn in Section VI.

II. PRELIMINARIES

In this section, we first introduce some background of polar encoding and then briefly describe the process of BP decoding. In addition, the definition of stopping trees is provided for polar codes.

A. POLAR CODES AND ENCODING

Let $F = \begin{bmatrix} 1 & 0 \\ 1 & 1 \end{bmatrix}$ denote the kernel matrix used for construction of polar codes. $F^{\otimes n}$ denotes the n -th Kronecker power of F , where $n = \log_2 N$ and N is the code length. Apply the transform $F^{\otimes n}$ to a block of N bits and then transmit the output bits through independent copies of a BDMC, call it W . Polar codes are constructed based on the general phenomenon, called channel polarization [1]. The channel polarization theorem states that as n goes to infinity, the bit channels start polarizing to either a pure-noise channel or a noiseless channel, where the fraction of noiseless channels is close to the capacity $I(W)$. Polar codes transmit information bits over the noiseless channels, while fixing the bits transmitted through the noisy ones to a value known to both the transmitter and the receiver. Correspondingly, an (N, K) polar code can be generated as follows: First, an N -bit sequence u_1^N is constructed by assigning K information bits to the positions corresponding to noiseless channels and “0” bits to rest $N - K$ positions corresponding to noise channels. Then, apply the polarization matrix $F^{\otimes n}$ to u_1^N and get an N -bit codeword c_1^N by

$$c_1^N = u_1^N F^{\otimes n}. \quad (1)$$

B. POLAR CODES BP DECODING

BP is a message passing decoding algorithm that has been widely used for decoding codes defined on graphs. Since polar codes can be represented in the form of a factor

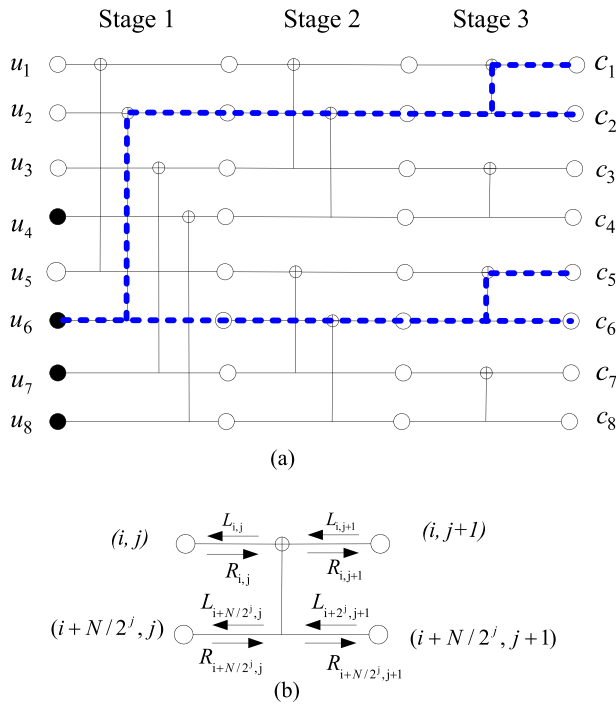


FIGURE 1. (a) BP factor graph of (8, 4) polar code. (b) Processing elements (PE) of the BP algorithm.

graph [9], BP decoding algorithm can be iteratively applied for polar code as well. A polar code with length N can be represented by an n -stage factor graph, which includes $N(n+1)$ nodes. BP runs on the factor graph in a stage-by-stage fashion. That is, BP runs on each stage of the adjacent check and variable nodes and then all parameters are passed to the next stage. In each iteration, message updates from the leftmost column to rightmost column. After arriving at the leftmost stage, the course is reversed from the leftmost column to the rightmost one. The decoding of polar codes is done by processing elements (PE), whose generation matrix is equal to F [24]. Figure 1 represents the factor graph of a polar code with $N = 2^n = 8$ ($n = 3$). In each stage, there are $N/2 = 4$ PEs.

Each node is associated with two types of messages: the left messages and the right messages. Let $L_{i,j}^t$ and $R_{i,j}^t$ denote the left and the right messages in the logarithmic likelihood ratio (LLR) form of the node $v(i, j)$, respectively, and t is the iteration number. The updating of LLRs through iterations can be described as follows:

$$\begin{aligned} L_{i,j}^t &= f(L_{i,j+1}^{t-1}, L_{i+N/2^j,j+1}^{t-1} + R_{i+N/2^j,j}^{t-1}) \\ L_{i+N/2^j,j}^t &= f(R_{i,j}^{t-1}, L_{i,j+1}^{t-1}) + L_{i+N/2^j,j+1}^{t-1} \\ R_{i,j+1}^t &= f(R_{i,j}^{t-1}, L_{i+N/2^j,j+1}^{t-1} + R_{i+N/2^j,j}^{t-1}) \\ R_{i+N/2^j,j+1}^t &= f(R_{i,j+1}^{t-1}, L_{i,j}^{t-1}) + R_{i+N/2^j,j}^{t-1} \end{aligned} \quad (2)$$

where $f(x, y) = \ln((1 + xy)/(x + y))$ denotes the propagation function to update messages. The function $f(\cdot)$ can be simplified by $f(x, y) \approx \text{sign}(x)\text{sign}(y) \min(|x|, |y|)$ for suiting

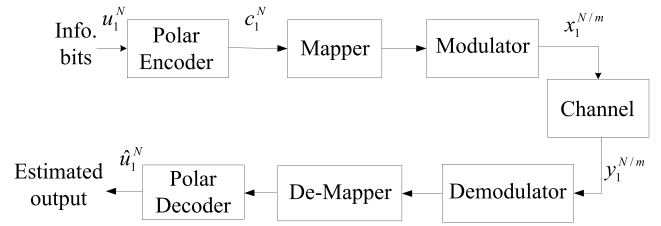


FIGURE 2. Block diagram of the proposed BIPCM system.

the hardware implementations [24]. Besides, much effort has been spent on polar codes with BP decoding for better performance [20], [25] and higher hardware efficiency [26].

C. STOPPING TREES

Stopping sets, as they contribute to the decoding failure, play an important role in error-correcting performance of the code [16]. An important category of stopping sets of polar codes is stopping tree. Stopping tree is rooted at (single) information bit (on the most left side of the factor graph), with leaves at coded bits (on the most right side of the factor graph). The set of leaf nodes of a stopping tree is referred to as the leaf-set of the tree, and the size of the leaf-set is referred to as leaf-set size. Figure 1 (a) shows an example of such a stopping tree with blue dotted lines. The information bit u_6 and the set $\{c_1, c_2, c_5, c_6\}$ are root node and corresponding leaf-set, respectively. In this example, the leaf-set size is 4. Every information bit has a unique stopping tree rooted at that information bit. Among all the stopping trees, the one with minimal leaf-set size is called a minimum stopping tree.

As proved by A. Eslami *et al.* in [17], [27], for two information bits with different leaf-set sizes, under BP decoding, the information bit with smaller leaf-set size is more likely to be erased than the one with larger leaf-set size. In the next section, the properties of polar codes over the factor graph will be used to optimize the combination of polar codes and BICM by designing an optimized mapping algorithm.

III. MAPPING DESIGN FOR BIPCM SYSTEMS

In this section, we first introduce the system model of the BIPCM, and then we propose a mapping design for the BIPCM where polar codes have already been given.

A. SYSTEM MODEL

The block diagram of the BIPCM system is shown in Figure 2, where the code length is N and a 2^m -ary modulation is adopted. We assumed that N is a multiple of m . Information bits sequence $u_1^N = (u_1, u_2, \dots, u_N)$ is fed to a polar encoder with a generator $F^{\otimes n}$ and encoded to a bit sequence $c_1^N = (c_1, c_2, \dots, c_N)$. Let X denote the signal space of 2^m -ary modulation. c_1^N is mapped into a 2^m -ary constellation symbol sequence $x_1^{N/m} = (x_1, x_2, \dots, x_{N/m})$ and each of the symbols

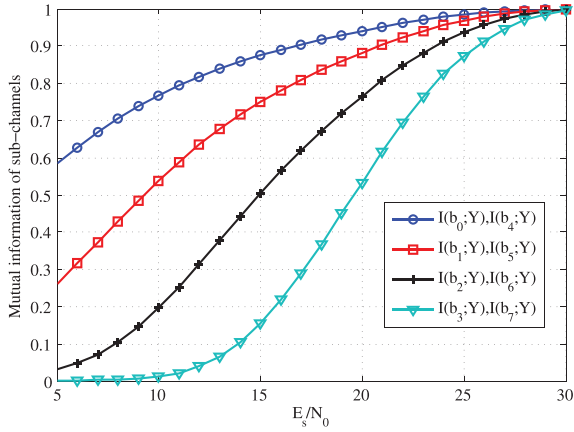


FIGURE 3. Sub-channel mutual information of 256-QAM with Gray labeling.

is drawn from X .¹ We denote the channel output by $y_1^{N/m} = (y_1, y_2, \dots, y_{N/m})$ with

$$y_l = x_l + n_l, \quad l \in 1, 2, \dots, N/m, \quad (3)$$

where $n_l = n_l^I + j \cdot n_l^Q$ is the white Gaussian noise, n_l^I and n_l^Q are independent Gaussian variables with mean 0 and variance $\sigma_n^2 = N_0/2$. For any $k \in \{1, 2, \dots, m\}$ and $x \in X$, the demodulator computes the LLR of the k -th coded bit of symbol x as

$$L_k(x) = \ln \frac{\sum_{x \in X_0^k} p(y|x)}{\sum_{x \in X_1^k} p(y|x)}, \quad (4)$$

where X_b^k is the subset of symbols $x \in X$ with the value $b \in \{0, 1\}$ at the k -th position, y is the channel output related to the codeword x through the conditional probability density function $p(y|x)$. These LLRs of coded bits are reordered by a de-mapper and fed to a polar decoder as the input message of the BP decoding to recover the information bits sequence u_1^N .

In a 2^m -ary BPCM system, the minimum Euclidean distance for each bit position of transmit symbol is different, which brings unequal error protections [8] for the m coded bits. The 2^m -ary input channel under BPCM is equivalent to a set of m independent parallel binary-input memoryless sub-channels under ideal interleaving. The mutual information of the k -th sub-channel with input b is given by

$$I_k(b; y) = 1 - E_{b,y} \left[\log_2 \frac{\sum_{x \in X} p(y|x)}{\sum_{x \in X_b^k} p(y|x)} \right], \quad (5)$$

where the expectation $E_{b,y}$ is calculated with $p(b) = 1/2$ and $p(y|b) = 2^{1-m} \sum_{x \in X_b^k} p(y|x)$. Figure 3 illustrates the mutual information of the 8 sub-channels for 256-QAM with Gray labeling. ch_3 , ch_7 , ch_2 and ch_6 have lower mutual information and the rest sub-channels have higher mutual information.

¹ Mapping in a 2^m -ary BPCM system refers to the rule assigning m coded bits to different bit positions of transmit symbols. While labelling denotes the rule assigning an m bits pattern to each transmit symbol, e.g. Gray labelling or anti-Gray labelling.

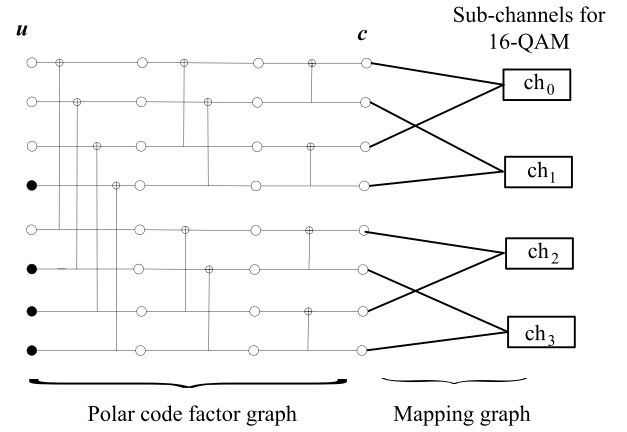


FIGURE 4. Polar coded BPCM graph.

B. MAPPING DESIGN FOR THE BPCM SYSTEM

Figure 4 shows a graph of the BPCM system, which consists of two bipartite graphs, namely, the polar code graph and the mapping graph between the coded bits and sub-channels. In the information updating process of BP decoding, each coded bit receives extrinsic information from the connected sub-channel. The coded bit transmitted over the sub-channel with lower reliability, has a higher probability to obtain an unreliable extrinsic information (and thus gets a LLR with very small absolute value). On the factor graph of the polar code, all leaf nodes of the polar code receive extrinsic information from the connected sub-channels, and then pass them in parallel from the leaf nodes (coded bits) to the root nodes (information bits). If all leaf nodes within a stopping tree corresponding to information u_i are transmitted over sub-channels with lower reliability, then there is minimal useful extrinsic information for the decoding process of \hat{u}_i , and thus \hat{u}_i will be wrongly decoded with a high probability. Therefore, in the designing of mapping rule, we need to separate sub-channels with lower reliability to different stopping trees, so that each stopping tree has at least one leaf node receiving reliable extrinsic information. Furthermore, based on the definition of the stopping tree, we refer to u_i as an unrecoverable root node (see Definition 1). The mapping rule is designed to minimize the number of unrecoverable root nodes.

To simplify the design, according to the mutual information of sub-channels, we divide all sub-channels into two groups: unreliable B containing the $m/2$ sub-channels with lower mutual information; and reliable G containing the rest $m/2$ sub-channels with higher mutual information. Next we present the following definitions referring to [28]. It should be noted that, the proposed mapping algorithm has a similar motivation as that of [28], that is providing more coding protection to coded bit that is less protected by the modulator. However, the reliability evaluation of coded bits of our mapping algorithm is different from that of [28].

Definition 1: A leaf node is a reliable leaf node if it is transmitted over a sub-channel in G and unreliable leaf node

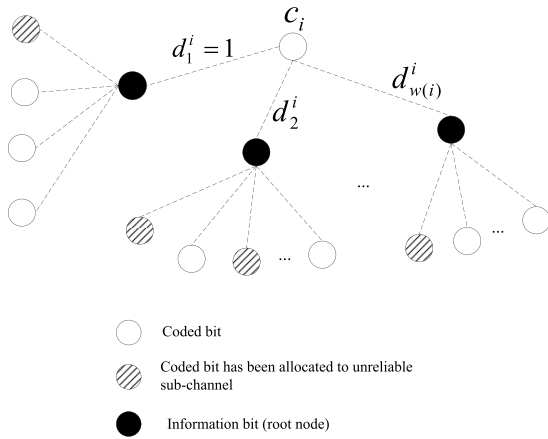


FIGURE 5. Subgraph spreading from the coded bit c_i .

if transmitted over the sub-channel in B ; A root node u_i is an unrecoverable root node if all leaf nodes in the stopping tree corresponding to u_i are unreliable leaf nodes, and otherwise u_i is a recoverable root node.

Definition 2: Figure 5 shows the sub-graph spreading for the leaf node c_i , $i \in [1, N]$. There are total $w(i)$ stopping trees with c_i being a leaf node, and the information bits shown in black circles denote the root nodes of these $w(i)$ stopping trees, respectively. If the ratio of unreliable leaf nodes among all leaf nodes in the j -th stopping tree is l , then we denote the j -th unreliable depth for leaf node c_i as $d_j^i = l$, $j \in [1, w(i)]$. Therefore, for each coded bit c_i , we use a $w(i)$ -tuple vector $D_i = \{d_1^i, d_2^i, \dots, d_{w(i)}^i\}$ to denote the unreliable depth profile of c_i .

Note that $w(i) + 1$ is in fact equal to the weight of the corresponding column of c_i in $F^{\otimes n}$. By the factor graph of polar codes, one can observe that one coded bit may be leaf node for more than one different stopping trees. We refer all leaf nodes within the same stopping tree as neighboring leaf nodes of each other. Let \bar{d}_i , described as

$$\bar{d}_i = \frac{1}{w(i)} \sum_{j=1}^{w(i)} d_j^i, \quad (6)$$

denote the average unreliable degree (AUD) of c_i . A relatively smaller \bar{d}_i means the extrinsic information from the coded bit c_i is relatively reliable, as the ratio of unreliable leaf nodes among all its neighboring leaf nodes is only \bar{d}_i . Therefore, the AUD \bar{d}_i measures the performance of a coded bit c_i . Besides, since a smaller AUD means less unreliable leaf nodes, it is less possible to produce unrecoverable root nodes if we transmit the coded bit with smaller AUD over the unreliable sub-channel.

For the 2^m -ary modulation, the set of coded bits mapped to 2^m -ary constellation symbol is partitioned into m subsets according to their positions within a transmitted symbol. For this reason, the overall coded bits of this transmission scheme may be partitioned into m subsets with size N/m . For $1 \leq k \leq m$, let C_k be the subset of the indices of the coded

Algorithm 1 Mapping Algorithm

```

1: Initialize:
2:  $C'_k \leftarrow \emptyset, k = 1, 2, \dots, m$ ;
3: Unallocated coded bits set  $V \leftarrow \{c_1, c_2, \dots, c_N\}$ ;
4: Allocated coded bits set  $A \leftarrow \emptyset$ ;
5:  $d_i^j \leftarrow 0, i = 1, \dots, w_j, \forall c_j \in V$ ;
6: Generator matrix of the polar code  $F^{\otimes n}$ .
7: for  $i = 1: m/2$  do
8:   for  $l = 1: N/m$  do
9:     if  $i = 1$  and  $k = 1$  then
10:      Select the coded bit which is present in the fewest
11:      number of stopping trees, for example  $c_j$ .
12:       $C'_i \leftarrow C'_i \cup c_j, V \leftarrow V \setminus c_j$ ,
13:       $A \leftarrow A \cup c_j, d_i^j \leftarrow \infty, i = 1, \dots, w(j)$ .
14:     else
15:       $\forall c_p \in V$ , calculate the AUD  $\bar{d}_p$ .
16:      Find the coded bit in  $V$  with the minimum
17:      AUD, for example  $c_o$ .
18:       $C'_i \leftarrow C'_i \cup c_o, V \leftarrow V \setminus c_o$ ,
19:       $A \leftarrow A \cup c_o, d_i^o \leftarrow \infty, i = 1, \dots, w(o)$ .
20:     end if
21:   end for
22: end for
23: for  $j = m : -1 : m/2 + 1$  do
24:   for  $l = 1: N/m$  do
25:     Find the unallocated coded bit with the maximum
26:     AUD, for example  $c_p$ .
27:      $C'_j \leftarrow C'_j \cup c_p, V \leftarrow V \setminus c_p$ .
28:   end for
29: end for
30: return  $(C'_1, C'_2, \dots, C'_m)$ .

```

bits transmitted over the k -th bit position of symbol. Sort all subsets in (C_1, C_2, \dots, C_m) in ascending order based on the reliability of the corresponding equivalent sub-channels and get $(C'_1, C'_2, \dots, C'_m)$. In particular, C'_1 and C'_m denote the subsets of coded bits corresponding to the least reliable bit positions and the most reliable bit positions, respectively. Next, we give the mapping design as follows to determine $(C'_1, C'_2, \dots, C'_m)$. Initialize $i = 1, j = m$ and $C'_k = \emptyset, k = 1, 2, \dots, m$.

- 1) Evaluate the reliability for each unallocated coded bit based on (6), then find the coded bit with the minimum AUD and put it into the set C'_i . Repeat this until the number of elements in C'_i is equal to N/m . Set $i = i + 1$;
- 2) Repeat 1) until $i = m/2 + 1$;
- 3) Find the coded bit with the maximum AUD and put it into the set C'_j . Repeat this until the number of elements in C'_j is equal to N/m . Set $j = j - 1$;
- 4) Repeat 3) until $j = m/2$.

The main loop of the mapping algorithm is given as Algorithm 1. Specifically, lines from 7 to 22 are determining coded bits transmitted over unreliable sub-channels, and lines from 23 to 29 are determining coded bits transmitted over

reliable sub-channels. It should be noted that all coded bits have the same initial AUD, i.e. 0, here we select the coded bit which is present in the fewest number of stopping trees as the first element of the first sub-set (see lines 10 and 11). That is because empirical results show that this coded bit is better protected than others in the factor graph [29]. For lines 16 and 17, if there is more than one coded bit with the minimum AUD, we group all the coded bits with the minimum AUD as a set U , then for each coded bit c_k in U , calculate the corresponding number of unrecoverable root nodes assuming that c_k is allocated to a sub-channel in B . Finally the coded bit corresponding to the minimum unrecoverable root nodes is selected. The computational complexity of the proposed mapping algorithm is at most $O(K \cdot N)$ which is bounded by $O(N^2)$.

In related works, a mapping algorithm is proposed in [20] for the concatenated polar codes with LDPC codes assuming that the outer LDPC code is regular with degree d_v . It should be noted that the mapping algorithm proposed in this paper differs from that in [20] mainly in two aspects: One is that the reliability evaluation method for coded bits is different. The d_v -tuple vector used in [20] can not be used to evaluate the reliability of coded bits for the polar coded BICM system since polar code is irregular. In this paper, based on the factor graph of polar codes, the AUD is originally proposed to evaluate the reliability of polar coded bit. The other one is the selection of the first element is different. For [20], the first element is selected randomly since all coded bits have the same initial reliability. Here, since all polar coded bits may have different initial reliabilities, the first element is selected according to the number of the involved stopping trees [29] for a better performance. Therefore, in this case the proposed mapping algorithm is an improved version of the mapping algorithm in [20].

IV. FLEXIBLE-LENGTH POLAR CODES

In the above section, Arkan's polar code is used for the BIPCM system, while assuming the code length N is a multiple of the modulation order m . However, the original polar codes with code length of $N = 2^n$ does not always match the code length requirement of the modulation. For example, codewords for 64-QAM should be in multiples of $m = 6$. There are three common types of used approaches to address this problem. The first approach is to use puncturing to get rate matching [5]. In addition, the second approach is to replace the 2×2 polar code basic matrix with the 3×3 basic matrix [30] or a mixture of variable-sized kernel matrices [4]. The third approach is to construct polar codes with flexible code length by coupling several short-length polar codes with simple operations like XORs and repetitions [31]. Here, we will follow the third approach: We propose a method to construct FLPC by coupling several original short length polar codes with a RA code. RA codes can be represented as a class of LDPC codes, and thus BP algorithm can be used to decode RA codes. The encoding/decoding algorithm of the proposed FLPC is described in the following paragraphs.

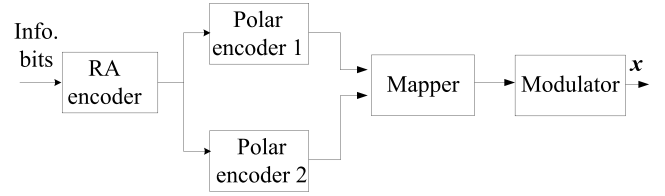


FIGURE 6. The encoder structure of the BIPCM system with FLPC.

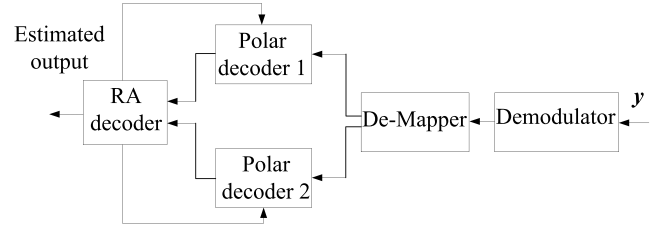


FIGURE 7. The decoder structure of the BIPCM system with FLPC.

A. ENCODING

The FLPC encoder includes a RA encoder and two short length polar encoders, as shown in Figure 6. A K_0 -bit information vector $u_1^{K_0}$ is encoded by an (N_0, K_0) RA encoder. An $(n = pK_0, K_0)$ RA code [23] is defined as follows. The information block of length K_0 is repeated p times, reordered by an interleaver of size pK_0 , and finally encoded by a rate one accumulator. Let $v_1^{N_0}$ denote the output of the RA encoder. Divide $v_1^{N_0}$ into two parts: $v_1^{K_1}$ and $v_{K_1+1}^{K_1+K_2}$, and send the two parts into polar encoder1 with (N_1, K_1) and polar encoder2 with (N_2, K_2) , respectively. The corresponding outputs are reordered by a mapper and mapped into 2^m -ary constellation symbols $x = (x_1, x_2, \dots, x_{\frac{N_1+N_2}{m}})$. The overall code length is $N_1 + N_2$ and the overall code rate is $R = \frac{K_0}{N_1+N_2}$. The generator matrices of the two polar codes are $H_1 = F^{\otimes n_1}$ and $H_2 = F^{\otimes n_2}$, respectively, where $n_1 = \log_2 N_1$ and $n_2 = \log_2 N_2$.

B. DECODING

Figure 7 shows the corresponding decoder structure of the FLPC. At the receiver BP decoding algorithm is exploited for both the polar and the RA codes in form of LLRs. More precisely, the demodulator computes the LLRs for each coded bit based on (4). Then, these bit LLRs are reordered by a de-mapper and fed to polar decoder1 and polar decoder2. For each iteration, the left messages of each polar code propagate from right to left until the stage 1, then these LLRs are passed to the RA decoder to perform the BP decoding. Furthermore, the output of the RA decoder is feedback to polar decoder1 and polar decoder2. Then for each polar decoder, the right messages propagate from left to right until reaching the most right stage. The decoding process continues until the maximum number of iterations is reached.

We note that the mapping rule, discussed in the above section, can be used for the BIPCM system with FLPC, as well, with only a slight special treatment for the selection

TABLE 1. Simulation parameters used for flexible-length polar codes.

code length	code rate	(N_0, K_0)	(N_1, K_1)	(N_2, K_2)
1536	1/2	(896, 768)	(1024, 598)	(512, 298)
1536	1/3	(768, 512)	(1024, 512)	(512, 256)
1280	1/3	(640, 426)	(1024, 512)	(256, 128)

of the most/least reliable bit. The modified mapping rule is given as follows: step 1

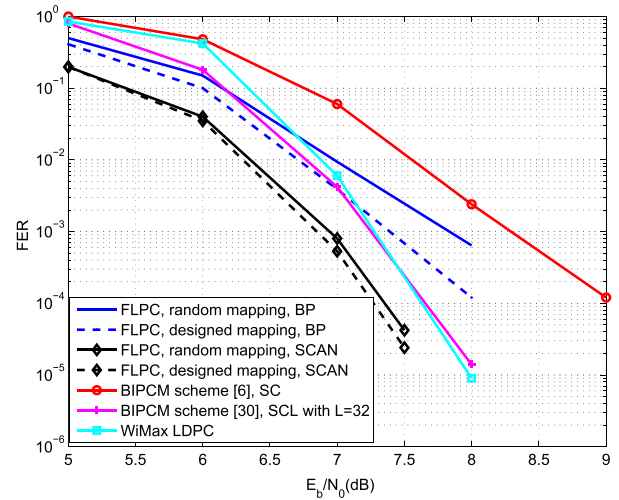
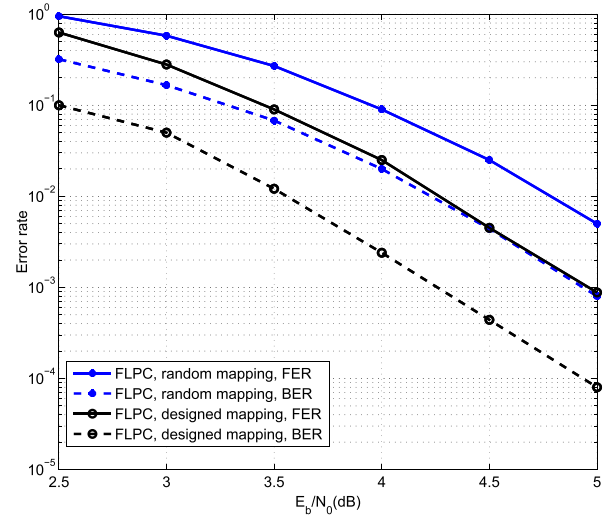
- 1) Evaluate the reliability for each unallocated coded bit of polar code 1 and polar code 2 based on (6), respectively. Find the coded bit with the minimum AUD and place it into the set C'_i .² Repeat this until the number of elements in C'_i reaches N/m . Set $i = i + 1$;
- 2) Repeat 1) until $i = m/2 + 1$;
- 3) Evaluate the reliability for each unallocated coded bit of polar code 1 and polar code 2 based on (6), respectively. Then find the coded bit with the maximum AUD and place it into the set C'_j . Repeat this until the number of elements in C'_j reaches N/m . Set $j = j - 1$;
- 4) Repeat 3) until $j = m/2$.

V. SIMULATION RESULTS

In this section, we provide some numerical results for the BIPCM system with the proposed mapping scheme to verify the accuracy of our theoretical analyses in Section III and Section IV. Figures 9-14 plot results over AWGN channels with all polar codes being constructed with the target $E_b/N_0 = 2\text{dB}$. The corresponding simulation parameters for FLPC are shown in Table 1. Besides, random mapping is employed as a baseline for comparison purposes, in which m bits are selected randomly from N coded bits and assigned to a transmitted symbol.

Figure 8 shows the frame error rate (FER) performance of the proposed FLPC over 64-QAM. Besides BP decoding, SCAN decoding is also considered for polar codes in FLPC and the maximum iteration is $I_{\max} = 15$. As a reference, the LDPC coded modulation scheme in WiMax with sum product algorithm, the BIPCM scheme with SC algorithm [6] and the one with CASCL algorithm [30] are also included in Figure 8. For the LDPC codes, the maximum number of iterations is 50. For the CASCL decoding, the list size is $L = 32$. As shown in Figure 8, the designed mapping has about 0.4dB gain at FER 10^{-3} comparing with the random mapping. With the designed mapping algorithm, the proposed FLPC scheme with BP decoding outperforms the BIPCM scheme with SC decoding [6] by up to 1dB. Moreover, the proposed mapping scheme can also bring performance gains for the FLPC system with SCAN decoding. With the help of SCAN decoding, the performance of the proposed FLPC scheme can outperform the BIPCM scheme

²Suppose the first polar code has Q_1 unallocated coded bits, and the second polar code has Q_2 unallocated coded bits. Evaluate reliability for each unallocated coded bit. Then select the coded bit with the minimum AUD among all the $Q_1 + Q_2$ coded bits.

**FIGURE 8.** Performance comparison over 64-QAM with Gray labeling between FLPC and other schemes. All schemes are with code length $N = 1536$ and code rate $R = 1/2$.**FIGURE 9.** FER performance of FLPC over 64-QAM with Gray labeling under BP decoding algorithm. $N = 1536$, $R = 1/3$ and $I_{\max} = 60$.

with CASCL decoding about 0.4dB. Apart from the faster convergence of SCAN, another possible reason for the good performance of the FLPC is that the combination of polar and RA codes forms a powerful concatenated scheme [17] to further push the error correction performance. Besides, Figure 9 and Figure 10 show the bit error rate (BER) and FER performance of the proposed FLPC over 64-QAM and 32-QAM, respectively. It is observed that the proposed mapping design offers up to 0.5dB gain comparing with the random mapping, which proves the effectiveness of the proposed mapping algorithm for the FLPC.

Figure 11 depicts the FER performance of polar codes over 16-ary pulse-amplitude modulation (PAM). As a reference, the performance of the maximum partial-polarization (MPP) mapping and channel mapping schemes shown in the figure are from Fig. 5 of [4] and Fig. 5 of [5], respectively. It is

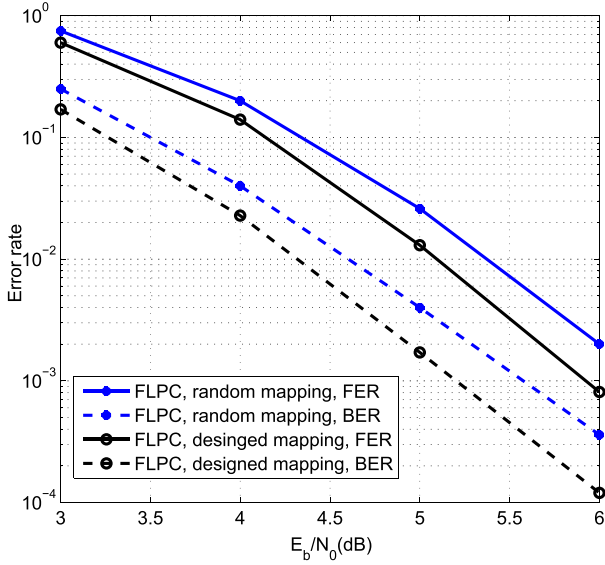


FIGURE 10. FER performance of FLPC over 32-QAM with Gray labeling under BP decoding algorithm. $N = 1280$, $R = 1/3$ and $I_{max} = 60$.

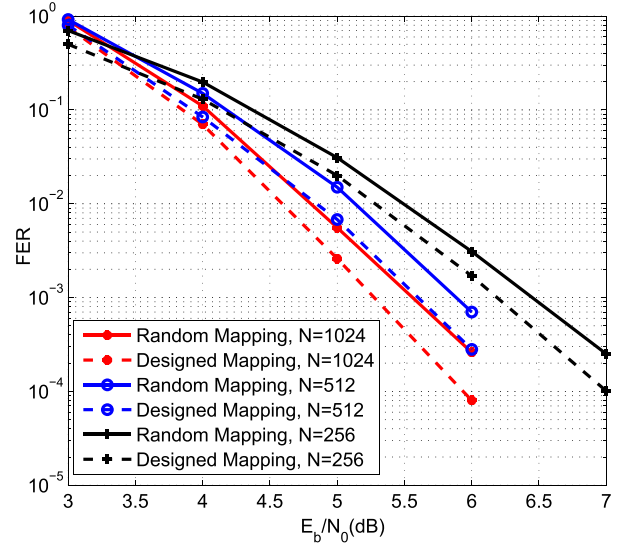


FIGURE 12. Performance of polar codes with different code lengths over 16-QAM with Gray labelling under BP decoding algorithm, $R = 1/2$ and $I_{max} = 60$.

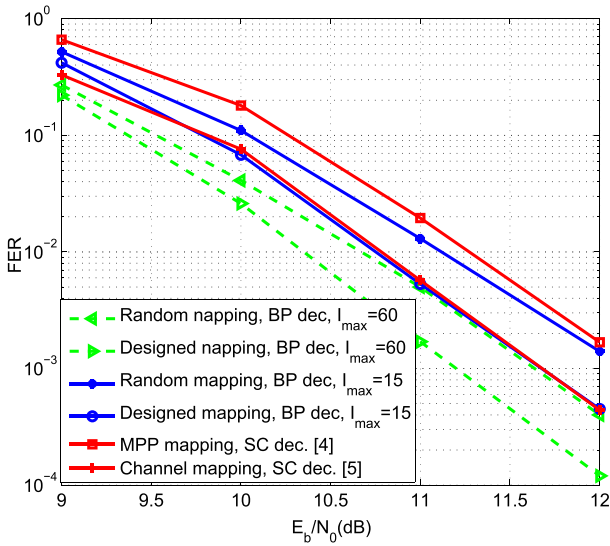


FIGURE 11. FER performance of polar codes over 16-PAM with Gray labelling under BP decoding algorithm, $N = 1024$, $R = 1/2$ and $I_{max} = 15, 60$.

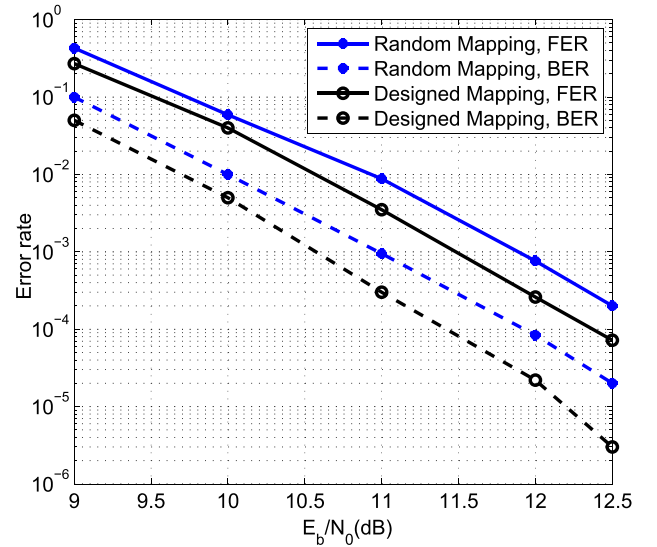


FIGURE 13. Performances of polar codes over 256-QAM with Gray labeling under BP decoding algorithm. $N = 1024$, $R = 1/2$ and $I_{max} = 60$.

observed that the designed mapping scheme with 15 iterations outperforms the MPP mapping scheme in [4] and shows a competitive FER performance compared to the scheme in [5]. However, the BP decoding with 15 maximal iterations has a higher throughput than the SC decoding [24]. Moreover, further increasing the iteration number of BP decoding provides much gain.

Figure 12 plots the performance of polar codes over 16-QAM with Gray labelling. Compared to the random mapping, the proposed mapping scheme provides a performance gain of about 0.2-0.25dB over that of a random mapping. As SNR increases, the performance gain becomes larger. Figure 13 shows the error rate for polar codes over 256-QAM.

Compared to the random mapping, the optimized mapping can improve the performance near 0.3dB and 0.4dB for the BIPCM scheme at FER 10^{-3} and BER 10^{-5} . Again the result shows the superiority of the proposed mapping rule over random mapping rule. Besides, as is described in Section III-B, less number of unrecoverable root nodes is desired for a good mapping scheme. We calculate the number of unrecoverable root nodes for different mapping schemes and find that the random mapping has unrecoverable root nodes while the designed mapping has no unrecoverable root node.

Figure 14 gives simulation results of polar codes over 16-QAM with natural labelling. It is observed that the proposed mapping exhibits an improvement of about 0.3dB

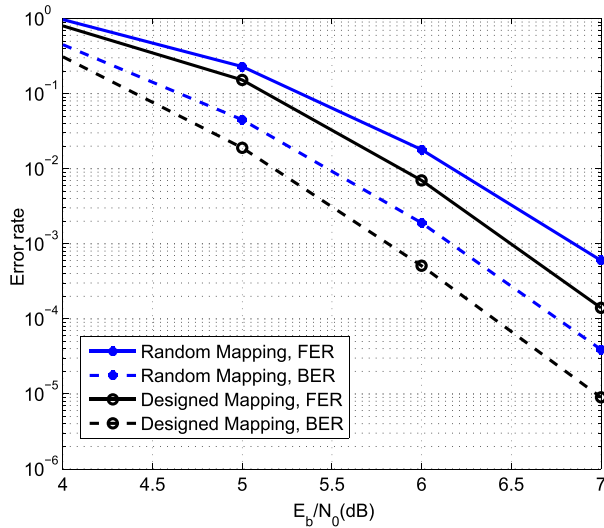


FIGURE 14. Performances of polar codes over 16-QAM with natural labelling under BP decoding. $N = 1024$, $R = 1/2$ and $I_{max} = 60$.

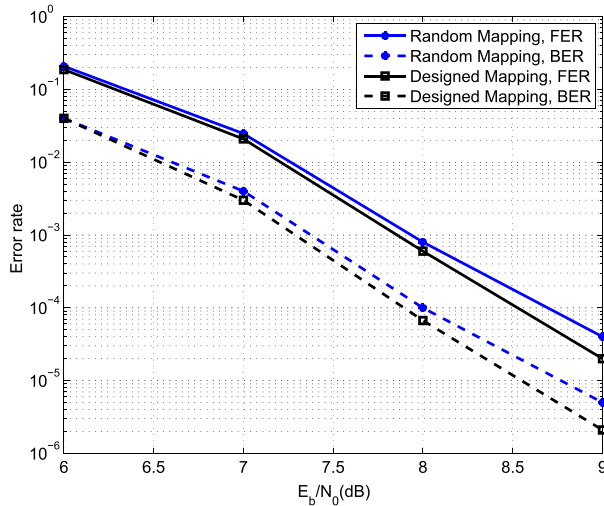


FIGURE 15. Performances of polar codes on Rayleigh fading channel over 16-QAM with Gray labelling under BP decoding. $N = 1024$, $R = 1/2$ and $I_{max} = 60$.

over random mapping at FER 10^{-3} . Furthermore, simulation results in Figures 14 and 12 demonstrate that the performance gain is greater with natural labelling than Gray labelling for polar codes with $N = 1024$. We analyze one possible reason is natural labelling owns lower reliable sub-channels, the proposed mapping weakens influence of them and thus brings a greater gain.

Next we give simulation results over fast fading channels in Figure 15. The fading channel is considered by $y = hx + n$, where y is the received symbol, x is the input symbol, h is picked from a Rayleigh distribution with $E\{|h|^2\} = 1$, and n is the additive complex Gaussian noise with zero mean and variance σ^2 . The random variable h is independent across transmissions, and it's assumed that a full channel state information is known at the receiver. Polar codes are

constructed using based on the equivalent AWGN channel with the same average mutual information [32]. It can be observed that the proposed mapping scheme can outperform the random mapping scheme. The results prove the efficiency of proposed mapping scheme in fading channels.

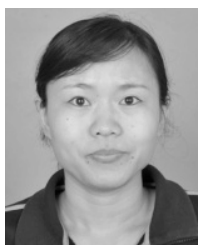
VI. CONCLUSION

In this paper, we considered the mapping design between coded bits and sub-channels of modulations for polar coded BICM schemes. We first proposed a two-layer bipartite graph to represent the polar coded BICM scheme. Then, we analyzed the stopping tree as well as the unequal protection of high level modulation, and investigated their effects on the BIPCM scheme. To this end, we considered using the known inequality in modulation protection of bits to improve the performance of BIPCM. Furthermore, a mapping algorithm which separates sub-channels with lower reliability to different stopping trees was proposed. The simulation results show that the proposed mapping scheme can achieve better BER and FER performance for finite length BIPCM systems in comparison to the traditional random mapping scheme, which will help to apply the polar coded modulation for practical wireless communication systems. Besides, we proposed the FLPC to meet the code-length requirements brought by the modulation order that is not a power of 2. With BP decoding algorithm, the performance of the proposed FLPC scheme with designed mapping can outperform the BIPCM scheme with SC decoding [6] by up to 1dB.

REFERENCES

- [1] E. Arikan, "Channel polarization: A method for constructing capacity-achieving codes for symmetric binary-input memoryless channels," *IEEE Trans. Inf. Theory*, vol. 55, no. 7, pp. 3051–3073, Jul. 2009.
- [2] Final Report of 3GPP TSG RAN WG1 #88 v1.0.0, document 3GPP TSG RAN WG1 #88bis, R1-1704172, Spokane, WA, USA, Apr. 2017.
- [3] M. Seidl, A. Schenk, C. Stierstorfer, and J. B. Huber, "Polar-coded modulation," *IEEE Trans. Commun.*, vol. 61, no. 10, pp. 4108–4119, Oct. 2013.
- [4] D.-M. Shin, S.-C. Lim, and K. Yang, "Mapping selection and code construction for 2^m -ary polar-coded modulation," *IEEE Commun. Lett.*, vol. 16, no. 6, pp. 905–908, Jun. 2012.
- [5] K. Chen, K. Niu, and J.-R. Lin, "An efficient design of bit-interleaved polar coded modulation," in *Proc. PIMRC*, Sep. 2013, pp. 693–697.
- [6] H. Mahdavi, M. El-Khamy, J. Lee, and I. Kang, "Polar coding for bit-interleaved coded modulation," *IEEE Trans. Veh. Technol.*, vol. 65, no. 5, pp. 3115–3127, May 2016.
- [7] D. Zhou, K. Niu, and C. Dong, "Universal construction for polar coded modulation," *IEEE Access*, vol. 6, pp. 57518–57525, 2018.
- [8] G. Caire, G. Taricco, and E. Biglieri, "Bit-interleaved coded modulation," *IEEE Trans. Inf. Theory*, vol. 44, no. 3, pp. 927–946, May 1998.
- [9] E. Arikan, "A performance comparison of polar codes and Reed-Muller codes," *IEEE Commun. Lett.*, vol. 12, no. 6, pp. 447–449, Jun. 2008.
- [10] N. Hussami, S. B. Korada, and R. Urbanke, "Performance of polar codes for channel and source coding," in *Proc. IEEE ISIT*, Jun. 2009, pp. 1488–1492.
- [11] S. M. Abbas, Y. Fan, J. Chen, and C.-Y. Tsui, "High-throughput and energy-efficient belief propagation polar code decoder," *IEEE Trans. Very Large Scale Integr. (VLSI) Syst.*, vol. 25, no. 3, pp. 1098–1111, Mar. 2017.
- [12] W.-C. Sun, W.-H. Wu, C.-H. Yang, and Y.-L. Ueng, "An iterative detection and decoding receiver for LDPC-coded MIMO systems," *IEEE Trans. Circuits Syst. I, Reg. Papers*, vol. 62, no. 10, pp. 2512–2522, Oct. 2015.

- [13] K. Lai, L. Wen, J. Lei, P. Xiao, A. Maaref, and M. A. Imran, "Sub-graph based joint sparse graph for sparse code multiple access systems," *IEEE Access*, vol. 6, pp. 25066–25080, 2018.
- [14] J. Yeo, S. Park, J. Oh, Y. Kim, and J. Lee, "Partial retransmission scheme for HARQ enhancement in 5G wireless communications," in *Proc. IEEE Globecom Workshops*, Dec. 2017, pp. 1–5.
- [15] A. Alvarado, L. Szczecinski, R. Feick, and L. Ahumada, "Distribution of L-values in Gray-mapped m^2 -QAM: Closed-form approximations and applications," *IEEE Trans. Commun.*, vol. 57, no. 7, pp. 2071–2079, Jul. 2009.
- [16] C. Di, D. Proietti, I. E. Telatar, T. J. Richardson, and R. L. Urbanke, "Finite-length analysis of low-density parity-check codes on the binary erasure channel," *IEEE Trans. Inf. Theory*, vol. 48, no. 6, pp. 1570–1579, Jun. 2002.
- [17] A. Eslami and H. Pishro-Nik, "On finite-length performance of polar codes: Stopping sets, error floor, and concatenated design," *IEEE Trans. Commun.*, vol. 61, no. 3, pp. 919–929, Mar. 2013.
- [18] B. Yuan and K. K. Parhi, "Architecture optimizations for BP polar decoders," in *Proc. IEEE ICASSP*, May 2013, pp. 2654–2658.
- [19] M. Mondelli, S. H. Hassani, and R. L. Urbanke, "From polar to Reed–Müller codes: A technique to improve the finite-length performance," *IEEE Trans. Commun.*, vol. 62, no. 9, pp. 3084–3091, Sep. 2014.
- [20] Q.-P. Yu, Z.-P. Shi, L. Deng, and X. Li, "An improved belief propagation decoding of concatenated polar codes with bit mapping," *IEEE Commun. Lett.*, vol. 22, no. 6, pp. 1160–1163, Jun. 2018.
- [21] S. M. Abbas, Y. Fan, J. Chen, and C. Tsui, "Concatenated LDPC-polar codes decoding through belief propagation," in *Proc. IEEE ISCAS*, May 2017, pp. 1–4.
- [22] F. Cheng, A. Liu, Q. Zhang, Y. Zhang, and B. Cai, "Codes design based on EXIT chart for polar coded BICM-ID," in *Proc. IEEE IAEAC*, Mar. 2017, pp. 1129–1133.
- [23] D. Divsalar, H. Jin, and R. J. McEliece, "Coding theorems for "turbo-like" codes," in *Proc. Annu. Allerton Conf. Commun. Control Comput.*, Sep. 1998, pp. 201–210.
- [24] Y. S. Park, Y. Tao, S. Sun, and Z. Zhang, "A 4.68 Gb/s belief propagation polar decoder with bit-splitting register file," in *Symp. VLSI Circuits Dig. Tech. Papers*, Jun. 2014, pp. 1–2.
- [25] U. U. Fayyaz and J. R. Barry, "Low-complexity soft-output decoding of polar codes," *IEEE J. Sel. Areas Commun.*, vol. 32, no. 5, pp. 958–966, May 2014.
- [26] K. Han, J. Wang, W. J. Gross, and J. Hu, "Stochastic bit-wise iterative decoding of polar codes," *IEEE Trans. Signal Process.*, vol. 67, no. 5, pp. 1138–1151, Mar. 2019.
- [27] A. Eslami and H. Pishro-Nik, "On bit error rate performance of polar codes in finite regime," in *Proc. 48th Annu. Allerton Conf. Commun., Control, Comput. (Allerton)*, Sep./Oct. 2010, pp. 188–194.
- [28] J. Du, J. Yuan, L. Zhou, and X. He, "A progressive edge growth algorithm for bit mapping design of LDPC coded BICM schemes," in *Proc. IEEE ISIT*, Jul. 2016, pp. 2129–2133.
- [29] A. Eslami and H. Pishro-Nik, "A practical approach to polar codes," in *Proc. ISIT*, Jul. 2011, pp. 16–20.
- [30] P. Chen, M. Xu, B. Bai, and X. Ma, "Design of polar coded 64-QAM," in *Proc. ISTC*, Sep. 2016, pp. 251–255.
- [31] *Channel Coding for Control Channels*, document 3GPP TSG RAN WG1 #86, R1-167216, Gothenburg, Sweden, Aug. 2016.
- [32] D. Zhou, K. Niu, and C. Dong, "Construction of polar codes in Rayleigh fading channel," *IEEE Commun. Lett.*, vol. 23, no. 3, pp. 402–405, Mar. 2019.



QINGPING YU is currently pursuing the Ph.D. degree with the National Key Laboratory of Communications, University of Electronic Science and Technology of China, Chengdu, China. Her current research interests include information theory, coding theory, and wireless communications.



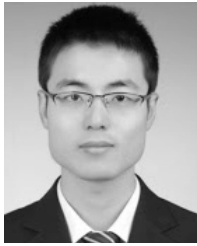
ZHIPING SHI received the master's and Ph.D. degrees from Southwest Jiaotong University, Chengdu, China, in 1998 and 2005, respectively. She has two years of a Postdoctoral experience with the University of Electronic Science and Technology of China (UESTC), from 2005 to 2007. She spent one year as a Visiting Scholar with Lehigh University, PA, USA, from 2009 to 2010. In 2007, she joined the School of Communication and Information with UESTC, where she is currently a Professor with the National Key Laboratory of Communications. Her research interests include in the areas of coding theory, cognitive radio wireless, and communication.



XINGWANG LI (S'12–M'15) received the B.Sc. degree in communication engineering from Henan Polytechnic University, Jiaozuo, China, in 2007, the M.Sc. degree from the National Key Laboratory of Science and Technology on Communications, University of Electronic Science and Technology of China (UESTC), and the Ph.D. degree in communication and information system from the State Key Laboratory of Networking and Switching Technology, Beijing University of Posts and Telecommunications (BUPT). He spent one year as a Visiting Scholar with the Institute of Electronics, Communications and Information Technology (ECIT), Queen's University Belfast (QUB), Belfast, U.K., from 2017 to 2018. He is currently a Lecturer with the School of Physics and Electronic Information Engineering, Henan Polytechnic University. He has several papers published in journal and conferences, has authored several patents. He has worked on several funded research projects on the wireless communications areas. His research interests include MIMO communication, cooperative communication, hardware constrained communication, non-orthogonal multiple access (NOMA), physical layer security, unmanned aerial vehicles (UAV), free space optical (FSO) communications, and performance analysis of fading channels.



MUHAMMAD ASIF received the B.S. degree in telecommunication engineering from the Islamia University of Bahawalpur, Pakistan, in 2013, and the M.S. degree in communication and information systems from Northwestern Polytechnical University, Xian, China, in 2015. He is currently pursuing the Ph.D. degree in communication and information systems with the University of Science and Technology of China, Hefei, China. His research interest includes channel coding, mainly for construction and decoding of QC-LDPC codes.



JIAYI ZHANG received the B.Sc. and Ph.D. degrees in communication engineering from Beijing Jiaotong University, China, in 2007 and 2014, respectively. From 2012 to 2013, he was a visiting Ph.D. student with the Wireless Group, University of Southampton, U.K. From 2014 to 2016, he was a Postdoctoral Research Associate with the Department of Electronic Engineering, Tsinghua University, China. From 2014 to 2015, he was a Humboldt Research Fellow with the Institute for Digital Communications, University of Erlangen–Nuremberg, Germany.

Since 2016, he has been a Professor with the School of Electronic and Information Engineering, Beijing Jiaotong University. His current research interests include massive MIMO, ad hoc networks, and the performance analysis of generalized fading channels. He was recognized as an Exemplary Reviewer of the IEEE COMMUNICATIONS LETTERS, in 2015 and 2016. He was also recognized as an Exemplary Reviewer of the IEEE TRANSACTIONS ON COMMUNICATIONS, in 2017. He serves as an Associate Editor of the IEEE COMMUNICATIONS Letters and IEEE ACCESS.



KHALED M. RABIE received the B.Sc. degree (Hons.) in electrical and electronic engineering from the University of Tripoli, Tripoli, Libya, in 2008, and the M.Sc. and Ph.D. degrees in communication engineering from the University of Manchester, Manchester, U.K., in 2010 and 2015, respectively. He is currently a Postdoctoral Research Associate with Manchester Metropolitan University (MMU), Manchester. His research interests include signal processing, and analysis of

power line and wireless communication networks. He was a recipient of the Best Student Paper Award at the IEEE ISPLC, TX, USA, 2015, and the MMU Outstanding Knowledge Exchange Project Award of 2016. He is the Program Chair of the IEEE ISPLC'18, the IEEE CSNDSP'18 Co-Chair of the Green Communications and Networks track and the Publicity Chair of the INISCOM'18. He is also an Associate Editor of IEEE ACCESS, an Editor of the *Physical Communication Journal* (Elsevier), and a Fellow of the U.K. Higher Education Academy (FHEA).

• • •